

PAPER • OPEN ACCESS

Development of 2024 AA-Yttrium composites by Spark Plasma Sintering

To cite this article: CH S Vidyasagar and D B Karunakar 2018 *IOP Conf. Ser.: Mater. Sci. Eng.* **346** 012050

View the [article online](#) for updates and enhancements.

You may also like

- [Spark plasma sintering of Inconel 738LC: densification and microstructural characteristics](#)
O F Ogunbiyi, E R Sadiku, T Jamiru et al.
- [A study of silicon carbide reinforced W-Ni-Cu based heavy alloys sintered with different heating modes](#)
A Raja Annamalai, Jitender Kumar Chaurasia, Muthe Srikanth et al.
- [Odyssey of thermoelectric materials: foundation of the complex structure](#)
Khalid Bin Masood, Pushpendra Kumar, R A Singh et al.



ECS
The
Electrochemical
Society
Advancing solid state &
electrochemical science & technology

DISCOVER
how sustainability
intersects with
electrochemistry & solid
state science research

Development of 2024 AA-Yttrium composites by Spark Plasma Sintering

CH S Vidyasagar¹ and D B Karunakar².

¹Metallurgical and Materials Engineering Department, Indian Institute of Technology Roorkee - 247667, India.

²Mechanical and Industrial Engineering Department, Indian Institute of Technology Roorkee - 247667, India.

Corresponding author (Email: bennyfme@iitr.ac.in).

Abstract

The method of fabrication of MMNCs is quite a challenge, which includes advanced processing techniques like Spark Plasma Sintering (SPS), etc. The objective of the present work is to fabricate aluminium based MMNCs with the addition of small amounts of yttrium using Spark Plasma Sintering and to evaluate their mechanical and microstructure properties. Samples of 2024 AA with yttrium ranging from 0.1% to 0.5 wt% are fabricated by Spark Plasma Sintering (SPS). Hardness of the samples is determined using Vickers hardness testing machine. The metallurgical characterization of the samples is evaluated by Optical Microscopy (OM), Field Emission Scanning Electron Microscopy (FE-SEM). Unreinforced 2024 AA sample is also fabricated as a benchmark to compare its properties with those of the composite developed. It is found that the yttrium addition increases the above mentioned properties by altering the precipitation kinetics and intermetallic formation to some extent and then decreases gradually when yttrium wt% increases beyond 0.3 wt%. High density (< 99.75) is achieved in the samples and highest hardness achieved is 114 Hv, fabricated by spark plasma sintering and uniform distribution of yttrium is observed.

Keywords: Spark plasma sintering, 2024 AA, Yttrium addition, Microstructure characterization, Mechanical properties.

1. Introduction

Industrial development of Al-based alloys is conservative because it is mostly concentrated on modifications of common and well known alloy systems (Al-Cu, Al-Si, Al-Mg-Si, Al-Zn-Mg, Al-Li-Cu, etc.) and processing routes. The reason is that there is a lack of experience in new alloy systems and production methods. However, standard systems stated above seem to approach their mechanical limits. Rapidly solidified (RS) alloys of non-conventional compositions recently attracted great interest, because they are able to achieve tensile strength exceeding 1000 MPa. In particular, RS Al-TM-based alloys (TM=transition metals, such as Fe, Ni, Cr, V, Zr, Ti, rare earth metals, etc.) with amorphous or nanocrystalline structure are of importance. It was reported that ultrahigh tensile strength levels above 1200 MPa, more than double that of the commercial high-strength Al alloys, were achieved for some fully amorphous RS Al-based alloys [1]. Yttrium plays a role similar to that of cerium. The beneficial effect of yttrium could be attributed to its high



oxygen affinity, which possibly helped forming a strong and adherent film. Certain metals that are difficult to be manufactured by other techniques can be shaped by powder metallurgy. Important applications of P/M include aerospace, automobile, lamp bulbs, oil-impregnated bearings, gears and filters [3]. High energy ball milling (HEBM) is an effective method of blending and alloying of the powders before consolidation [4].

Spark plasma sintering (SPS) is a novel method for consolidating nanocrystalline materials with stunted grain growth and effective shrinkage in less time as well as obtaining cleaner grain boundaries for effective interface formation [2, 5]. The success of spark plasma sintering is usually related to its higher heating rates and shorter holding times and the properties of the component are higher compared to hot pressing [6-9]. This method is very promising, especially for ceramics, due to its ability to create nanoscale size grains [10, 11] and to retain original properties [9, 12, 13], with application to metal-matrix composites. Several recent studies have shown that the SPS method allows many properties to be improved. Kurita et al. [14] produced multi-walled carbon nanotube reinforced aluminium matrix composite with an ultimate tensile strength that was 4 times higher than that of the pure aluminium. Ullbrand et al. [7] showed that, by means of SPS instead of hot pressing, a stronger adhesion could be obtained between the matrix and the reinforcement. Long et al. [15] produced composites with a micro hardness that was 3.5 times higher than those produced by classical sintering method. The current plays two roles in SPS i.e. source of heating by Joule's effect and promoter of enhanced diffusion rate during phase growth and intermetallic diffusion [16]. The production techniques have led to an unprecedented growth in the area of metal matrix composites with extraordinary superior strengths by necessary dislocations [16]. However, the fundamental mechanism of the SPS method is still unclear though different mechanisms have been proposed [17]. Alternative explanations to the plasma effect have been proposed, for example rapid Joule heating, local melting or particle deformation [18].

Lim [19] reported the combined effect of grain refiners Al-5Ti-1B (fixed at 0.1wt% Ti and 0.02wt% B) and yttrium on the mechanical properties of A356 gravity die castings and found that 0.3 wt% yttrium addition renders the highest hardness value of 23.88 HRA (60kgf), a 20% improvement, compared to A356. However, the improvement of other mechanical properties was not significant compared to other reinforcement and processing techniques. Hui-Zhong [20] found that the addition of 0.10% Y could speed up the age hardening of 2519 alloy. The tensile strength was increased by 5 MPa with peak ageing at room temperature. Addition of 0.20% Y makes the tensile strength of the alloy to reach 205 MPa at 300 °C, which is 30% higher than that of the alloy without Y addition. However, the author did not report the influence of Y on the mechanical properties at room temperature. Cooke et.al [21] fabricated 2024 AA powders with the addition of 0.1, 0.2, and 0.4 wt% scandium by SPS. However, yield strength, ultimate tensile strength and ductility of the alloy did not increase significantly and the 2024 AA reinforced with TM like RE was investigated by very few researchers. This research aims to evaluate the microstructure and mechanical properties of 2024 AA reinforced with different percentages of Y ranging from 0.1 to 0.5 wt% using SPS.

2. Experimental work

2.1 Materials and methods

In this work, the materials chosen are 2024 aluminium alloy and yttrium. Since the available literature is limited, some preliminary experiments are conducted to assess the feasibility of fabricating aluminium-yttrium composite by Spark Plasma Sintering. The chemical composition of as-received aluminium 2024 alloy is shown in Table 1. The average particle size is 60 microns.

Table 1 Chemical composition of as- received Al 2024 alloy.

Element	Si	Cu	Fe	Zn	Mg	Ti	V	Mn	Al
Wt%	0.16	4.67	0.47	0.14	1.71	0.05	0.001	0.80	balance

Five samples alloyed with different amounts of Y are developed. This powder was produced at AlfaAesar (United States) through nitrogen atomization.

2.2 High energy mechanical ball milling (HEMBM)

Yttrium particles of size 40 mesh of one dimensional nano size are used for reinforcement. Planetary ball mill is used for uniform mixing of both the powders. The ball mill is rotated at a speed of 50 rpm for 2 hours and thus a uniform powder of the alloy is prepared as starting powder material. The as-received powders are analysed by scanning electron microscope (SEM), as shown in figure 1 (a) and (b).

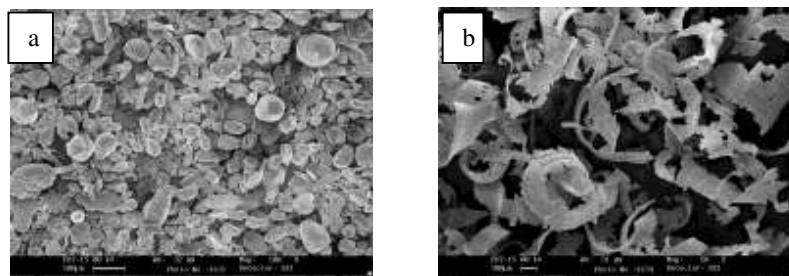
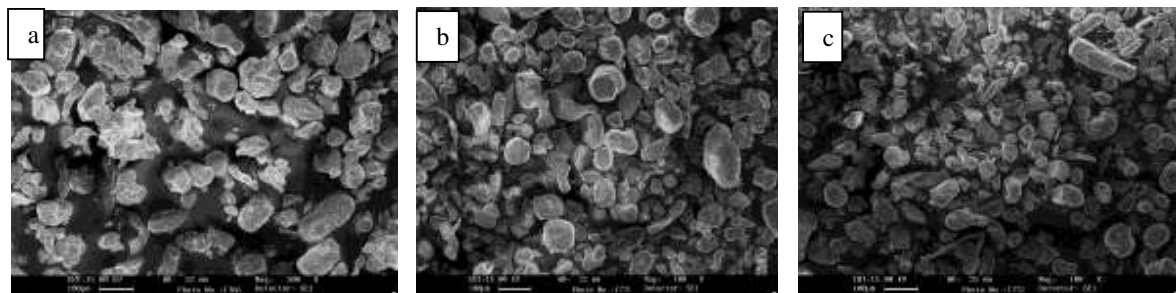


Fig. 1. SEM of experimental powders (a) 2024 AA and(b) Yttrium

From the SEM analysis it is evident that the average particle size of 2024 AA is around 60 microns and yttrium is one dimensional nano flakes of size 40 mesh. But after blending of both the powders by ballmilling, there are no traces of flakes except a few small ones here and there by which it can be concluded that the one dimensional flakes have been milled down to nano size. Figure 2 shows the SEM images of the milled powders.



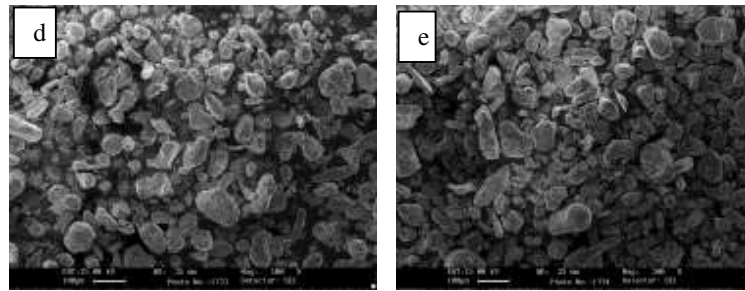


Fig.2. SEM images of the blended powders (a) with 0.1 wt % Y, (b) with 0.2 wt % Y, (c) 0.3 wt % Y, (d) with 0.4 wt % Y and (e) with 0.5 wt % Y.

Even if the very small percentage of yttrium has not been in the focus of SEM, we can clearly assume that in at least one image the flakes would have appeared. We can also observe that the flakes were cracked initially before milling and were prone to break easily due to increase in ball to powder ratio (4:1)

2.3 Spark plasma sintering

The blended powders are then sieved and processed by SPS at the following parameters.

1. Temperature – 450 °C.
2. Rate of temperature rise – 50°C/ minutes.
3. Pressure – 50 MPa.
4. Holding time – 180 seconds.

The samples prepared by SPS are shown in Figure 3, starting from pure 2024AA to 2024AA + 0.5wt%Y.



Fig 3. SPSed samples with different proportions of wt % Y.

3. Results and discussion

3.1 Microstructure

The aluminium matrix being very soft, polishing of the sample for microscopy results in removal of reinforcement particles from the matrix and also leaves marks on the surface of the sample. From the microstructure, we can observe the reduction in grain size as the wt% of Y increases and it is clear that the grain sizes of reinforced samples are smaller than that of the non reinforced alloy. Beyond 0.3wt% Y the grain size tends to grow, as shown in figure 4 (a), (b), (c), (d), (e) and (f). However, the grain size change is not a clear evidence to the changes in properties. Yttrium

addition accelerate the precipitation kinetic of Al-Cu alloys [20]. So, the precipitation of Cu with Al forming Al_2Cu played an important role in strengthening the composites.

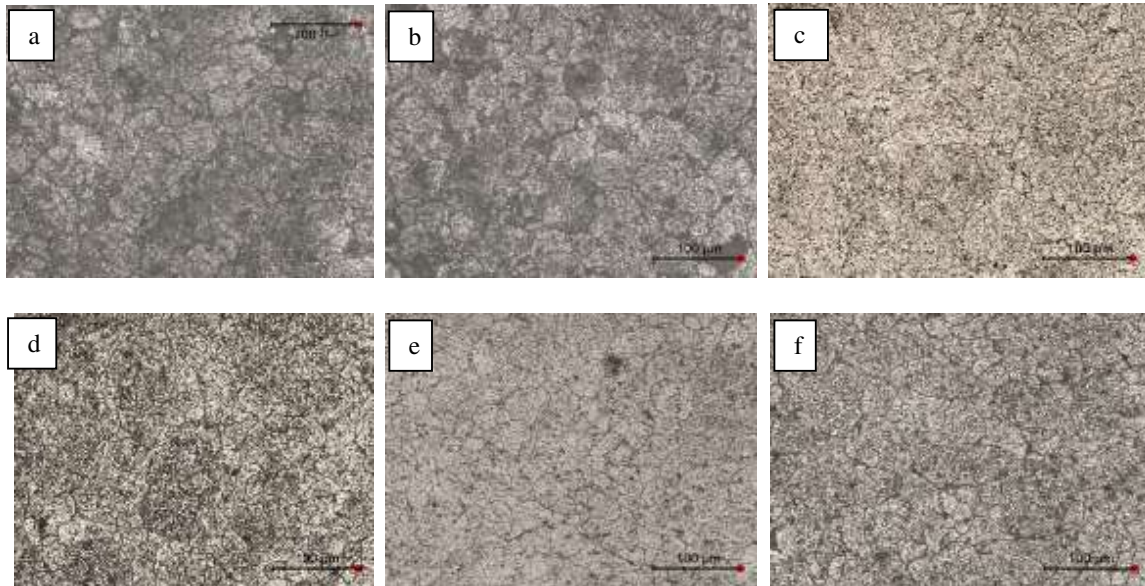


Fig 4. Microstructure of the samples(a) with 0.0 wt % Y, (b) with 0.1 wt % Y, (c) with 0.2 wt % Y, (d) 0.3 wt % Y, (e) with 0.4 wt % Y and (f) with 0.5 wt % Y.

3.2 FE-SEM analysis

The samples are also examined by FE-SEM and EDS. The results showed traces of yttrium present in very small amount and uniformly distributed. The results are shown in figure 5. We can see good interface bonding and a few surface pores as well.

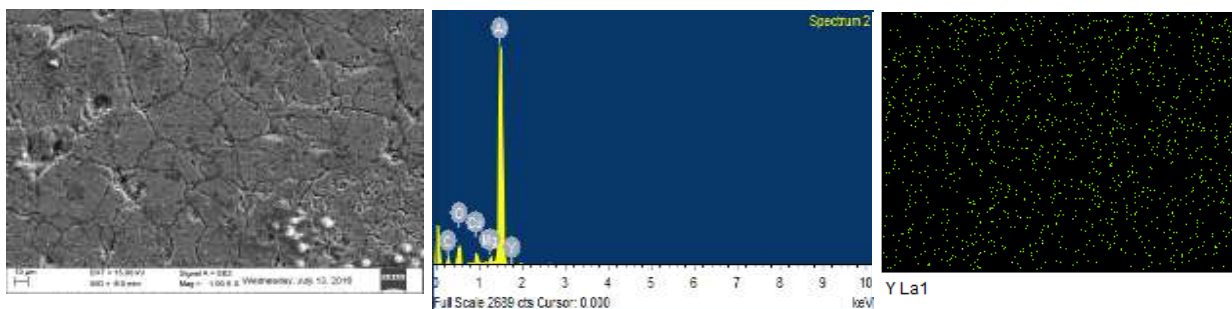


Fig. 5 .FE-SEM and corresponding EDS of 0.3 wt% Y.

3.3 Density calculation

By SPS almost fully dense samples were obtained but as the Y wt% increases beyond 0.3% the density saturates. The percentage yttrium versus theoretical densities, experimental densities and relative densities of the samples are shown in the figure 6. The experimental densities are calculated using standard Archimedes principle. The high density achieved was by adopting appropriate SPS parameters.

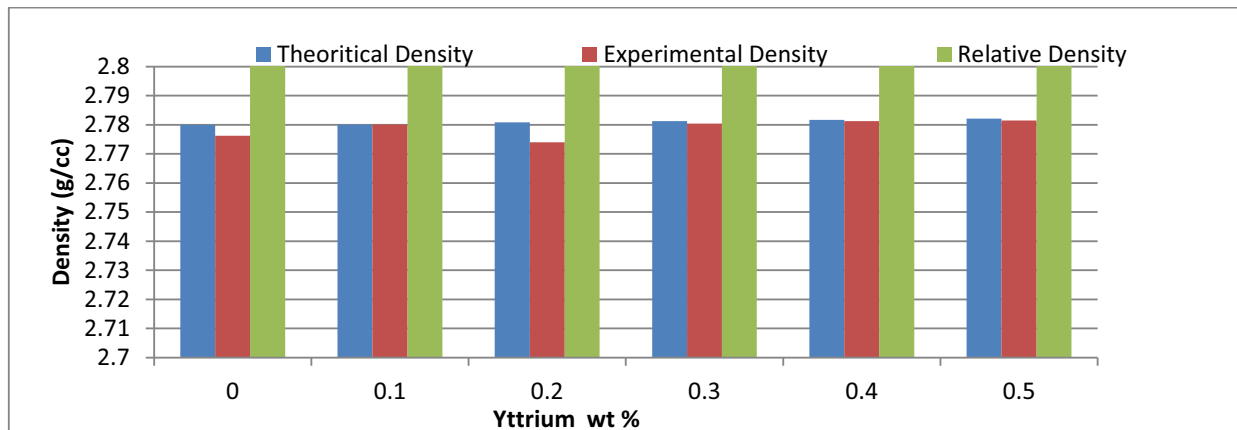


Fig. 6. Variation of actual, experimental and relative densities with respect to wt% Y

3.4 Hardness

Hardness is measured by Vickers hardness testing machine with 5 Kg load. Due to the high density of the samples, considerably good hardness is achieved but after 3 wt% Y the hardness tends to decrease as shown in figure 6. The main strengthening mechanism involved is the formation of Al-Cu precipitates which decrease as the Yttrium is increased beyond 0.3. This phenomenon occurs due to the formation of Al-Cu-Y intermetallics at the grain boundaries. However, in alloys without copper content only intermetallic phase Al-y aggregates along grain boundaries and hence enhances grain boundaries to resist slipping or dislocation [22]. Beyond 0.3 wt% Y which the amount of Al-Cu precipitates decreases in the samples.

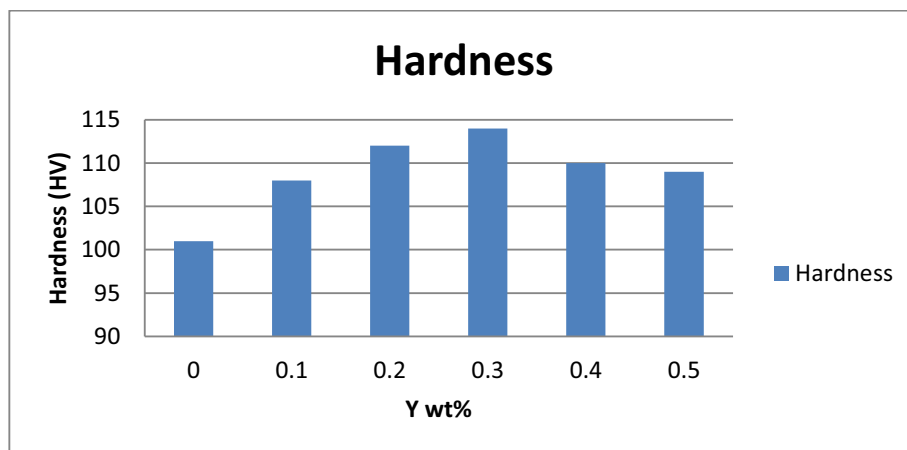


Fig. 7. Variation of hardness with yttrium wt%.

4. Conclusions

Based on the present work, the following conclusions can be drawn:

1. Five different composites of 2024 AA + Y with different weight percents of Y were successfully fabricated by SPS with densities more than 99%. The high density attributes to the tight packing of powder particles by appropriate SPS parameters.

2. It is observed that the precipitation of Cu played an important role in strengthening the composite. Yttrium addition accelerated the precipitation kinetics upto 0.3 wt% but, beyond 0.3 wt% it forms an intermetallic with Al and Cu and thus decreases the Cu precipitation.
3. FE-SEM and EDS analysis show the presence of yttrium at uniform distribution, which enhances the mechanical properties. Hence, ball milling may be treated as an appropriate mean of blending powders.
4. Due to the high density of the samples considerably good hardness is achieved but after 0.3 wt% Y the hardness tends to decrease and the highest hardness registered is 114 HV.

References

- [1] Vojtech D. Challenges for research and development of new Aluminium alloys. *Metabk*, 49(3) (2010) 181-185.
- [2] Olivier Guillon, Jesus Gonzalez-Julian, Benjamin Dargatz, Tobias Kessel, Gabi Schierning, Jan Rathel, Mathias Herrmann. Field – Assisted sintering technology / Spark Plasma Sintering: Mechanisms, Materials, and Technology Developments. *Advanced Engineering Materials* 2014, 16, 830-850.
- [3] Goetzel CG. Dispersion strengthened alloy: The possibilities for light metals. *Mod Dev. Powder Metall.* 4, (1971) 425.
- [4] Flores MI. Comparative study of al-ni-mo alloys obtained by mechanical alloying in different ball mills. *Rev. Adv. Mater. Sci.* 18 (2008), 301.
- [5] Handwerker CA, Cahn JW, Manning JR. Thermodynamics and Kinetics of Reactions at Interfaces in Composites. *Mater Sci Eng. A* 126 (1990) 173–189.
- [6] Munir ZA, Anselmi-Tamburini U, Ohyanagi M. The effect of electric field and pressure on the synthesis and consolidation of materials: A review of the spark plasma sintering method. *J Mater Science* (2006) 41763–777.
- [7] Ullbrand JM, Cordoba JM, Tamayo-Ariztondo JM, Elizalde MR, Nygren M, Molina-Aldareguia JM, Oden M. Thermo-mechanical properties of copper-carbon nanofibre composites prepared by spark plasma sintering and hot pressing *Compos. Sci Technol* 70 (2010) 2263–2268.
- [8] Daffos B, Chevallier G, Estournes C, Simon P. Pulse analysis and electric contact measurements in spark plasma sintering. *Power Source* (2011) 196. 1620–1625.
- [9] Jain D, Reddy KM, Mukhopadhyay A, Basu B. Mater Achieving uniform microstructure and superior mechanical properties in ultrafine grained TiB₂- TiSi₂ composites using innovative multi stage spark plasma sintering. *Sci Eng A* 528, (2010) 200–207.
- [10] Hungria T, Galy J, Castro A. Spark plasma sintering a useful technique to the nanostructuration of piezo-ferroelectric materials. *Adv Eng Mater.* 11 (2009) 615–631.
- [11] Yar MA, Wahlberg S, Bergqvist H, Salem HG, Johnsson M, Muhammed M. Chemically produced nanostructured ODS–lanthanum oxide–tungstencomposites sintered by spark plasma. *Nucl J. Mater* 408(2011) 129–135.
- [12] Dumont-Botto E, Bourbon C, Patoux S, Rozier P, Dolle M. Synthesis by Spark Plasma Sintering: a new way to obtain electrode materials for lithium ion batteries. *J Power Sources* 196:2274–2278.

- [13] Okinaka N, Zhang L, Akiyama T. Thermoelectric Properties of Rare Earth-doped SrTiO₃ Using Combination of Combustion Synthesis (CS) and Spark Plasma Sintering (SPS). *ISIJ Int* 50 (2010) 1300–1304.
- [14] Kurita H, Kwon H, Estili M, Kawasaki A. Multi walled carbon nanotube-Aluminium matrix composites prepared by combustion of hetero-agglomeration method, Spark plasma sintering and hot extrusion. *Mater Trans* 52(10) (2011) 1960–1965.
- [15] Long BD, Othman R, Umemoto M, Zuhailawati H. Spark plasma sintering of mechanically alloyed in situ copper-niobium carbide composite. *Alloy J. Compd.* 505 (2010) 510–515.
- [16] Tan Z, Li Z, Fan G, Kai X, Ji G, Zhang J, Zhang D. Fabrication of diamond/aluminium composites by vacuum hot pressing: Process optimization and thermal properties. *Compos. B*, 47 (2013) 173–180.
- [17] Hulbert DM, Anders A, Dudina DV, Andersson J, Jiang D, Unuvar C, Anselmi-Tamburini. The absence of plasma in ‘spark plasma sintering’. *J. Appl. Phys.* 104(3), 033305/ 033301-033307 (2008).
- [18] Eriksson M, Shen Z, Nygren M. Fast densification and deformation of titanium powder. *Powder Metal* 48, (2005) 231–236.
- [19] Lim YP, Ooi JB, Wang X. Microstructural and mechanical properties of gravity-die-cast A356 alloy inoculated with yttrium and Al-Ti-B grain refiner simultaneously. *Archives of Foundry Engineering ISSN Volume 11 Issue 4*, (2011) 1897-3310.
- [20] Hui-Zhong LI, Liang Xiao-Peng, Li Fang-Fang Guo Fei-Fei, Zhou LI, Zhang Xin-Ming. Effect of Y content on microstructure and mechanical properties of 2519 aluminium alloy. *Transactions of nonferrous metal society of China*. Volume 17, Issue 6, (2007) 1194-1198.
- [21] Cooke RW, Kraus NP, Bishop DP. Spark plasma sintering of aluminum powders prealloyed with scandium additions. *Materials Science&Engineering A*. 657, (2016) 71–81.
- [22] Chen Yu-Yong, Si Yu-Feng, Kong Fan-Tao, Et Al. “Effects of yttrium on microstructures and properties of Ti-17Al-27Nb alloy”. *Transaction of Nonferrous Metals Society of China*, Vol 16, 2006, pp. 316-320.